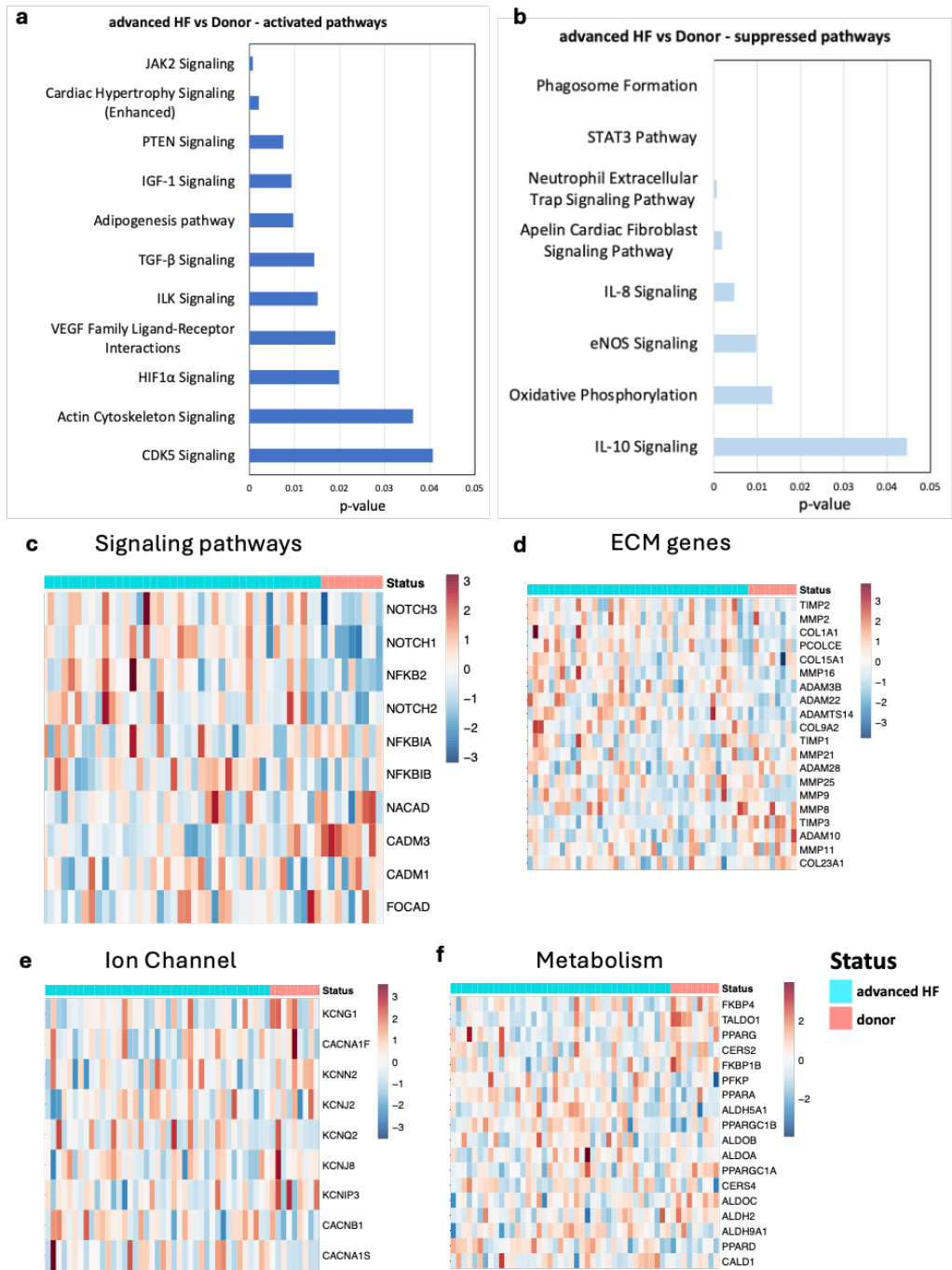
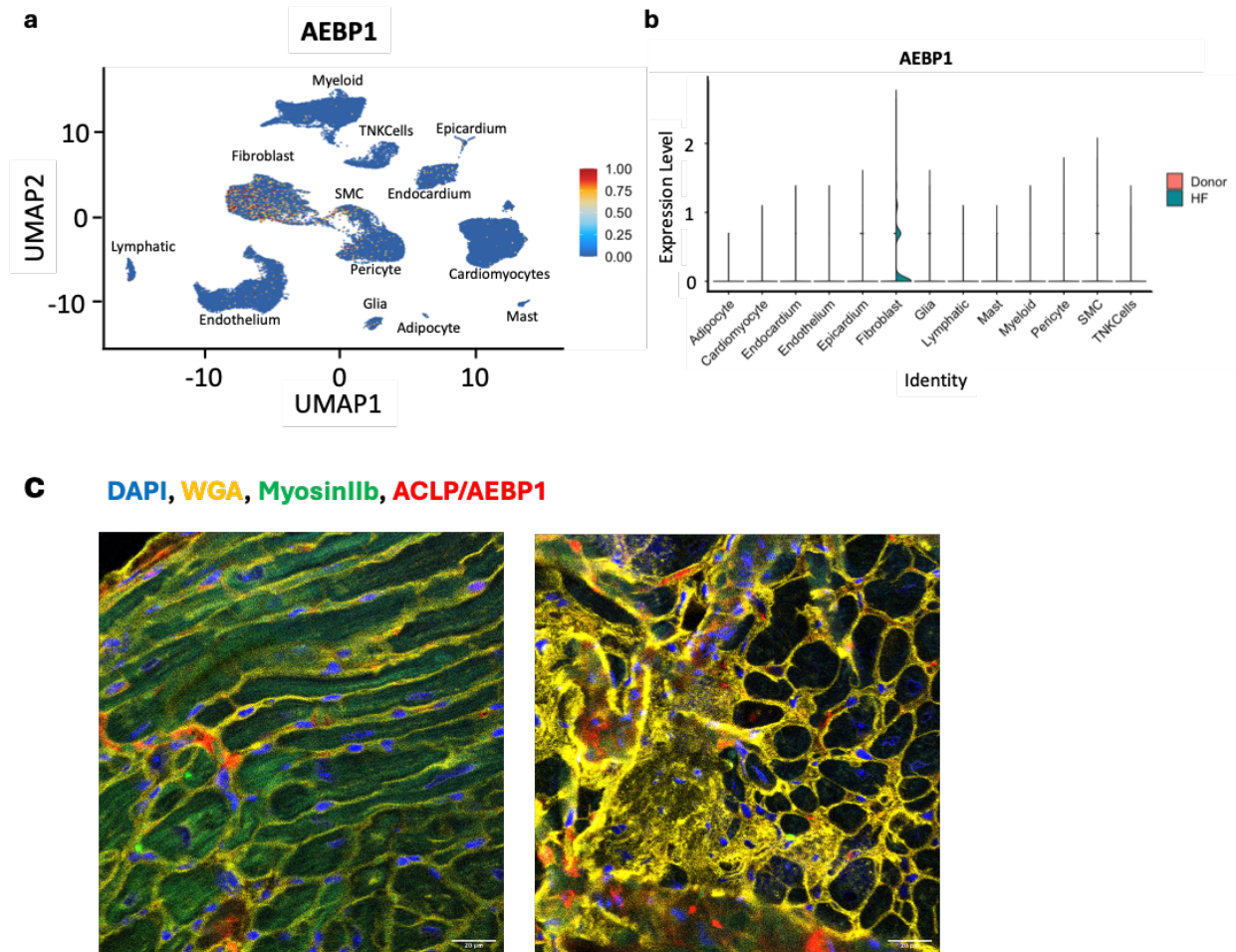


## Supplemental Figures and legends.

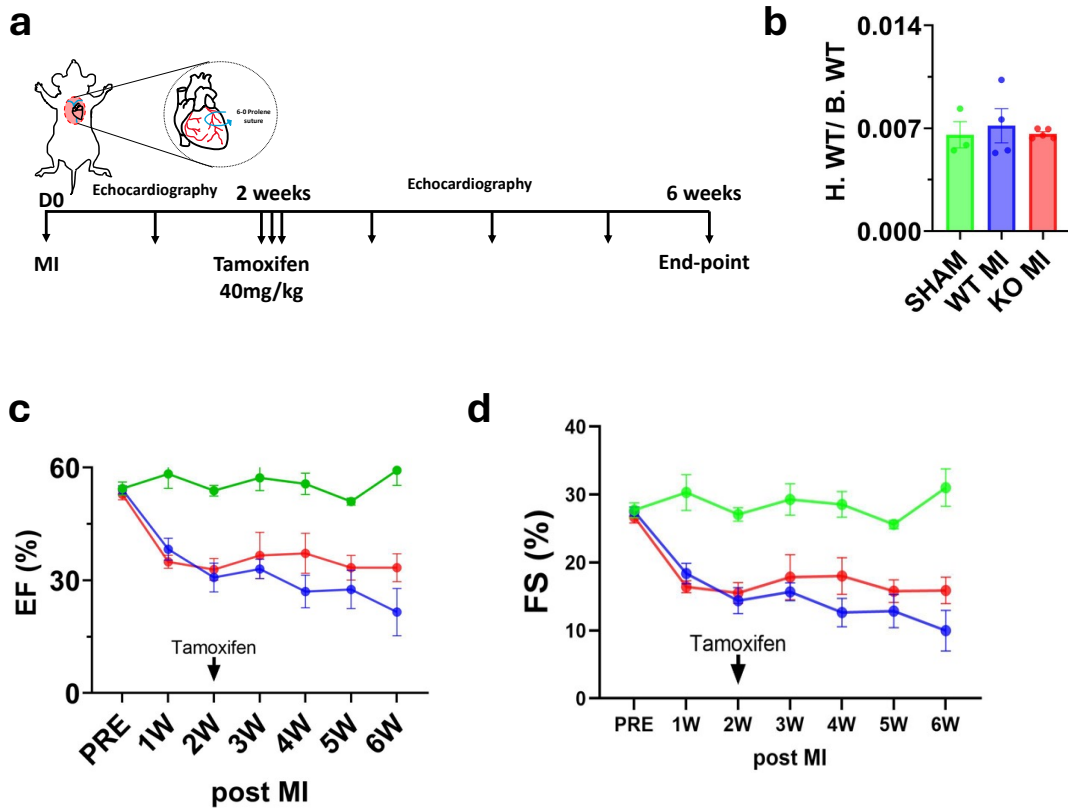


**Supplemental Fig. 1: a-b,** Ingenuity pathway analysis showing activated and suppressed pathways in advanced HF myocardium compared to non-failing donor myocardium (n=9 donor,

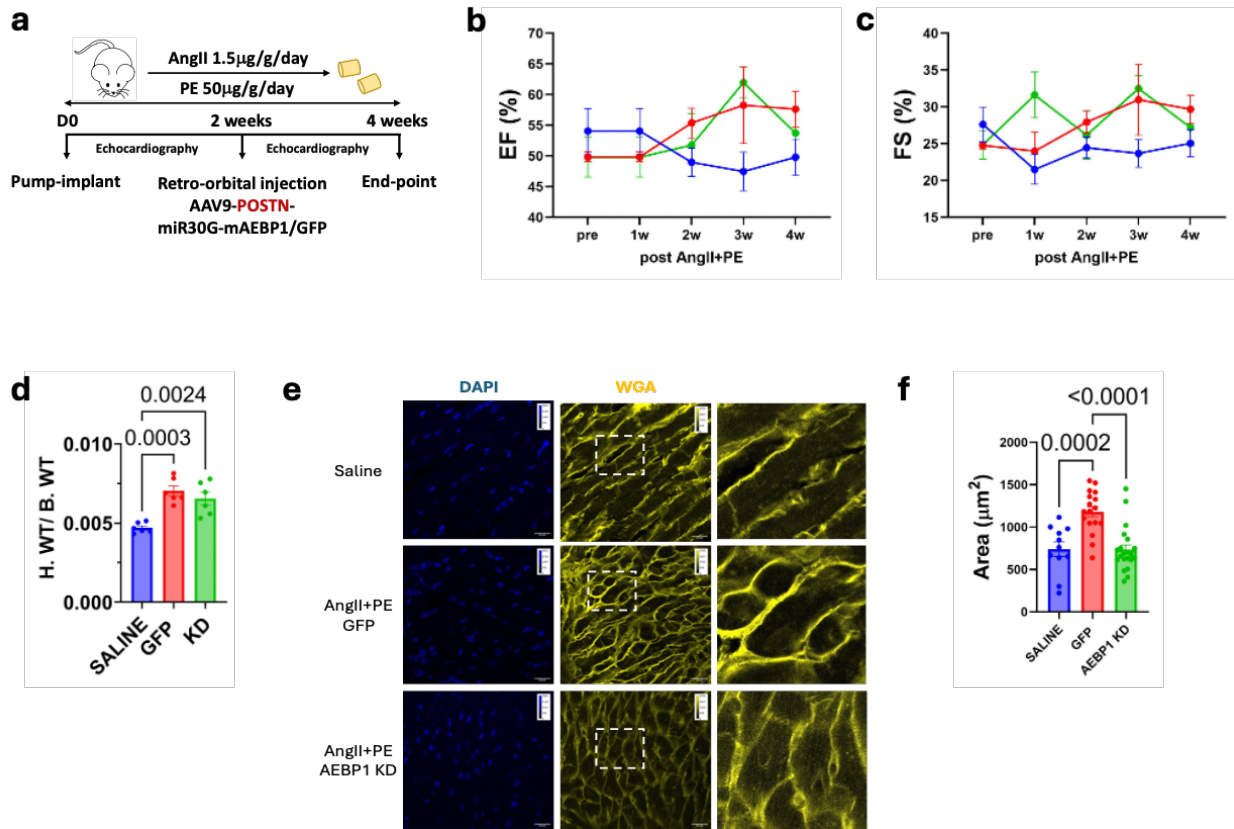
n=41 HF). **c-f**, Heat map of genes involved in cell signaling pathways, ECM organization, Ion channel physiology, and metabolism respectively (n=9 donor, n=41 HF).



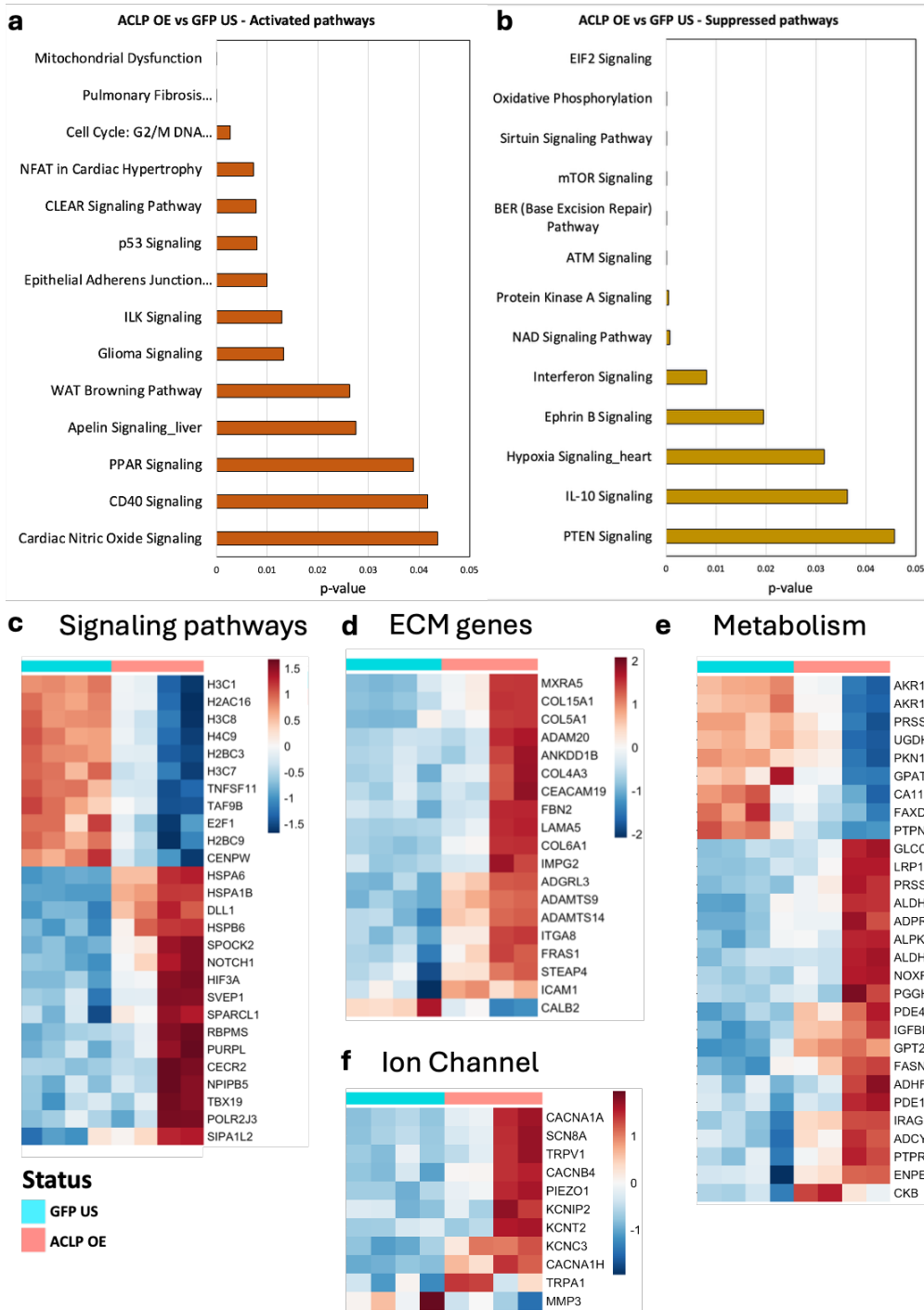
**Supplemental Fig. 2:** **a**, Single-nuclear RNA sequencing (snRNA seq) data showing *AEBP1* expression in human non-failing donor myocardium across different cell types (n=14 donor). **b**, Violin plot of snRNA seq showing differential expression of *AEBP1* between donor and HF myocardium across cell types (n=14 donor, n=13 HF). **c**, Representative immunohistochemistry image on mouse myocardium 4days post-MI (n=3).



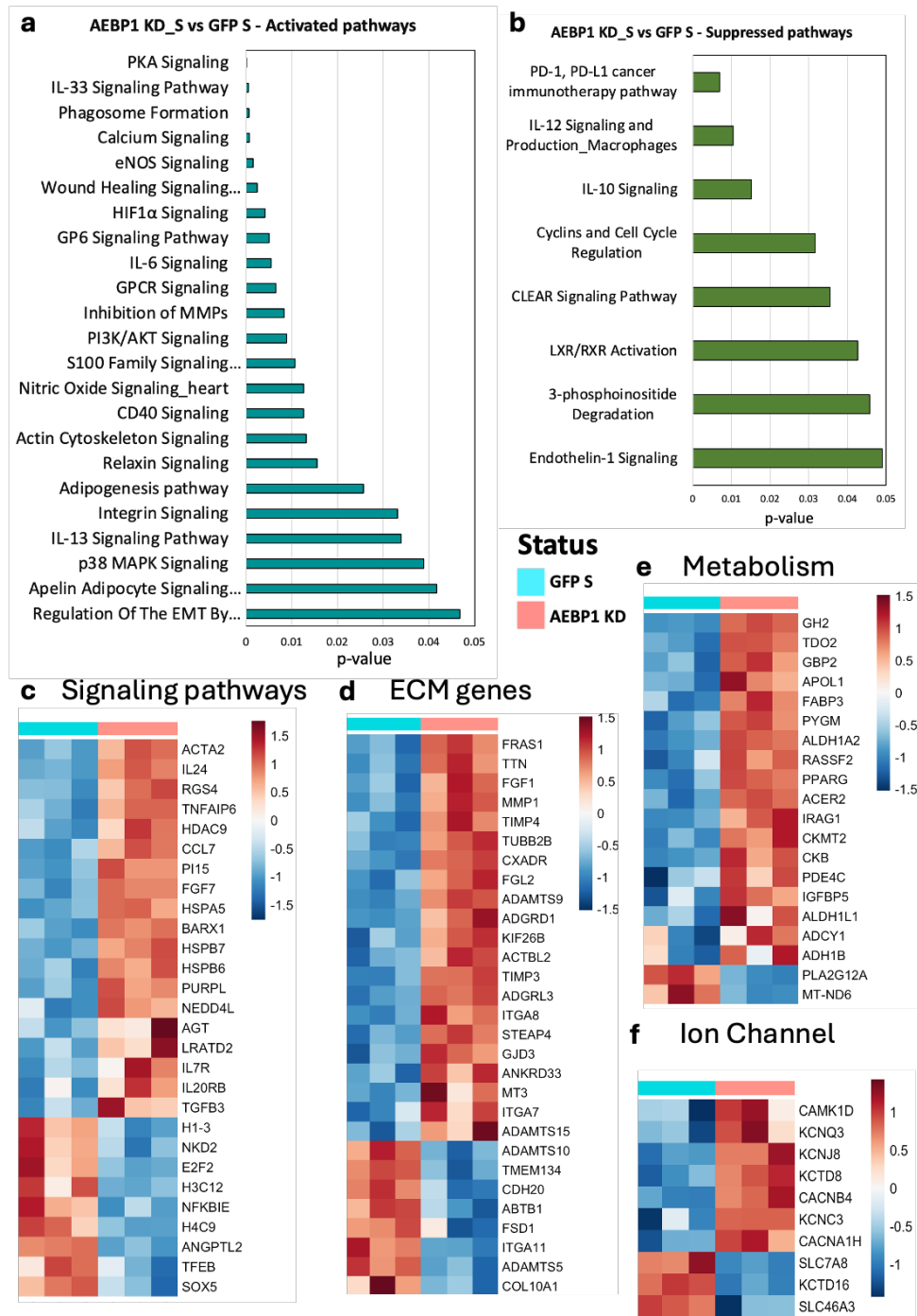
**Supplemental Fig. 3: a**, Schematic of heart failure induction and fibroblast-specific *Aebp1* KO. **b**, Heart weight to body weight ratio (n=3 Sham, n=4 WT MI, n=5 KO MI). **c-d**, Ejection fraction (EF%) and fractional shortening (FS%) data (n=3 Sham, n=4 WT MI, n=5 KO MI).



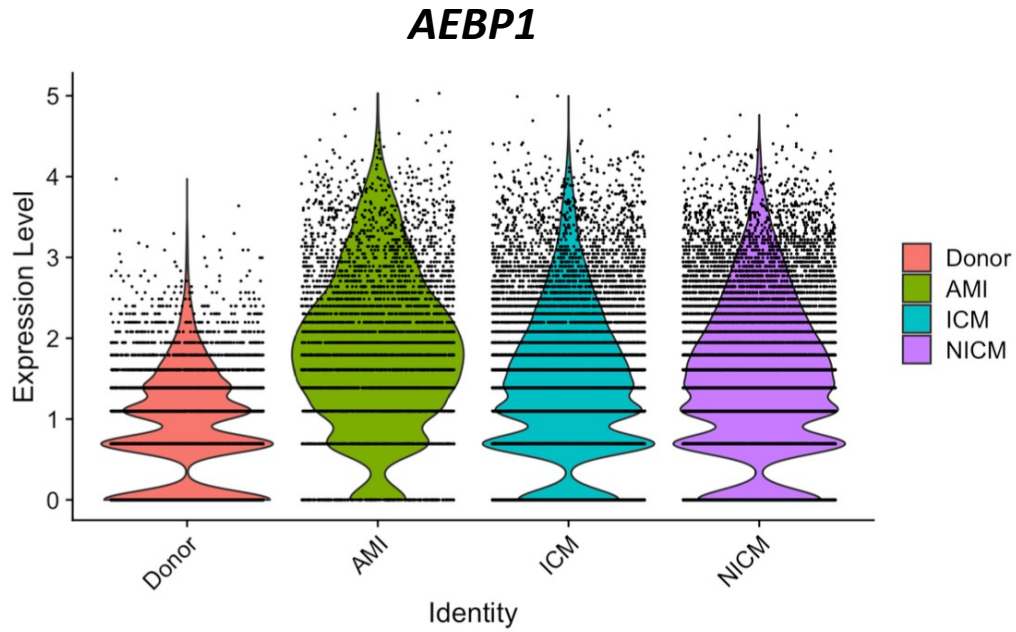
**Supplemental Fig. 4:** **a**, Schematic of AngII/PE infusion and fibroblast-specific *Aebp1* KD using AAV9. **b-c**, Ejection fraction (EF%) and fractional shortening (FS%) data (n=6 each). **d**, Heart weight to body weight ratio (n=6 each). **e**, Representative immunohistochemistry data (n=6 each). **f**, Cell surface area quantification (n=6 mice, multiple images/animal). p-value: One way ANOVA.



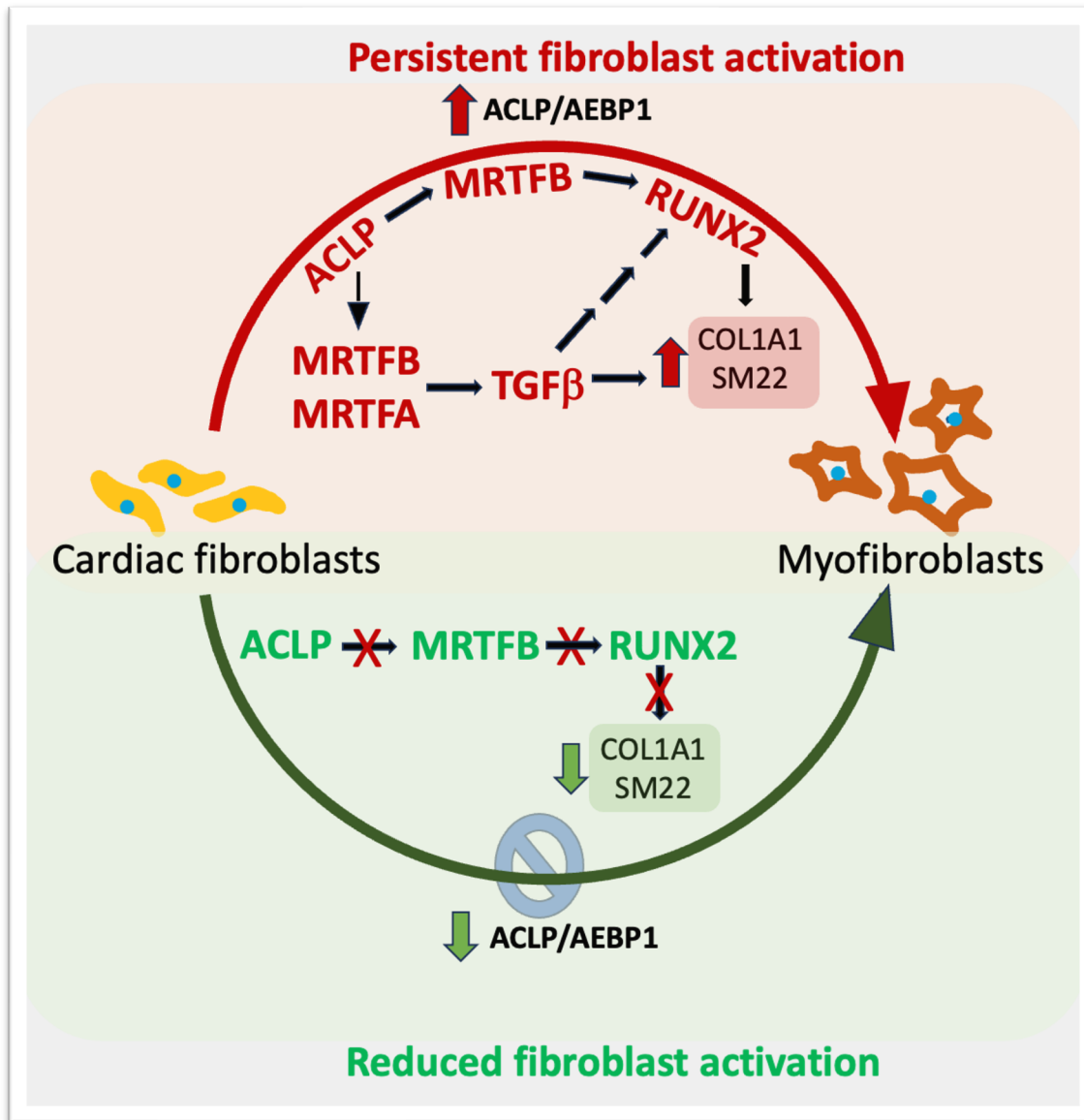
**Supplemental Fig. 5: a-b,** Ingenuity pathway analysis of RNA sequencing data from HCF following ACLP overexpression compared to unstimulated (US – no TGF-beta) GFP (n=4 each). **c-f,** Heat maps of genes involved in cell signaling, ECM organization, metabolism and ion channel signaling respectively (n=4 each).



**Supplemental Fig.6: a-b**, Ingenuity pathway analysis of RNA sequencing data from HCF following *AEBP1* KD compared to GFP S (S - TGF $\beta$  stimulated) (n=3 each). **c-f**, Heat maps of genes involved in cell signaling, ECM organization, metabolism and ion channel signaling respectively (n=3 each).



**Supplemental Fig. 7:** CITE-Seq data from non-failing donor (n=6), patient with acute myocardial infarction (AMI, n=4) and chronic HF (ICM- ischemic cardiomyopathy (n=6) and NICM- non-ischemic cardiomyopathy (n=6)) showing *AEBP1* expression in fibroblasts.



**Supplemental Fig. 8:** Elevated ACLP/AEBP1 expression promotes cardiac fibroblast activation through MRTFB- and RUNX2-dependent signaling pathway. RUNX2 activation leads to increased SM22 and COL1A1 production, whereas AEBP1 knockdown (KD) suppressed fibroblast activation by inhibiting both RUNX2 and MRTFB. RUNX2 KD suppressed SM22 and COL1A1 secretion without altering MRTFB levels, suggesting RUNX2 functions downstream of ACLP/AEBP1 signaling. These findings support the existence of an ACLP-RUNX2, ACLP-MRTFB or integrated ACLP-MRTFB-RUNX2 signaling cascade driving cardiac fibroblast

activation. Overall, the data identify AEBP1 inhibition as a potential therapeutic strategy for cardiac fibrosis attenuation.